

Washington University in St. Louis

Washington University Open Scholarship

Mechanical Engineering and Materials Science
Independent Study

Mechanical Engineering & Materials Science

5-10-2019

Heterogeneity and Elastic Microstructure Observed in 3 Orthogonal Faces of Metallic Glass, VIT106a

Raymond Condon

Washington University in St. Louis

Katharine Flores

Washington University in St. Louis

Follow this and additional works at: <https://openscholarship.wustl.edu/mems500>

Recommended Citation

Condon, Raymond and Flores, Katharine, "Heterogeneity and Elastic Microstructure Observed in 3 Orthogonal Faces of Metallic Glass, VIT106a" (2019). *Mechanical Engineering and Materials Science Independent Study*. 90.

<https://openscholarship.wustl.edu/mems500/90>

This Final Report is brought to you for free and open access by the Mechanical Engineering & Materials Science at Washington University Open Scholarship. It has been accepted for inclusion in Mechanical Engineering and Materials Science Independent Study by an authorized administrator of Washington University Open Scholarship. For more information, please contact digital@wumail.wustl.edu.

HETEROGENEITY AND ELASTIC MICROSTRUCTURE OBSERVED IN 3 ORTHOGONAL FACES OF METALLIC GLASS, VIT106A

Raymond Condon¹

Undergraduate Research Assistant
Email: rcondon@wustl.edu

Katharine M. Flores²

Professor, Director of ISME
The Flores Research Group
Department of Mechanical Engineering
Washington University in St. Louis
St. Louis, MO 63130
Email: floresk@wustl.edu

ABSTRACT

Heterogeneities in a molded cast plate of Vit106a ($Zr_{58.5}Cu_{15.6}Ni_{12.8}Al_{10.3}Nb_{2.8}$) were investigated on three orthogonal surfaces of the sample. Dynamic modulus mapping (DMM) and nanoindentation measurements were collected through the use of a nanoindenter and were consequently analyzed in MATLAB. All three faces revealed elastic variations, which were categorized into compliant, intermediate and stiff modulus categories. By constructing maps of the longitudinal section of the plate and comparing these maps to the transverse sections, unique directional alignment due to features of the mold surface that this bulk metallic glass (BMG) was originally in contact with during preparation was apparent. The dynamic modulus mapping revealed variations in the storage moduli on all three faces. The nanoindentation revealed slight variations in the reduced moduli and hardness in the various indent locations on each face.

NOMENCLATURE

E_r'	Storage Modulus
E_r''	Loss Modulus
E_r^*	Complex Modulus
E_r	Reduced modulus

1. INTRODUCTION

Crystal nucleation and growth in undercooled liquid alloys such as the Vit106a specimen in question have shown to display exceptional glass forming abilities when processed correctly. A glass is essentially a liquid that can “freeze” without crystallization. The crystals form from nucleation and growth. In theory, any metal can form a glass if it is cooled quick enough below its melting point. [1] Metals crystallize quickly as opposed to silicates, which are a typical type of glass. David Turnbull revealed that if the glass transition temperature is 2/3 of the melting point you should have glass formation. Essentially, anything will become a glass if it is cooled quick enough. If the ratio is 2/3, you do not have to cool it very fast at all. These eutectic bulk metallic glasses are interesting to study since they do not require extremely fast cooling rates.[2]

Specifically, these bulk metallic glasses have high toughnesses and yield strengths, which is why these materials are being researched. Interestingly, when bending these extremely thin samples of BMGs in tension, they shear band. You do not want to use metallic glass in tensile loading because it will experience wall slipping. Phone cases are being made out of these BMGs because when

a cell phone is dropped, you want the case to be able to bend and not break. There is not a lot of tensile ductility in these BMGs but they do have a high amount of toughness. [3]

Crystalline alloys tend to be very structured, whereas metallic glasses are amorphous and appear to be homogenous and isotropic when examined through traditional characterization methods. On very small length scales, metallic glasses are showing heterogeneities with varying properties in clustered regions. [4]

In this research, dynamic modulus mapping (DMM) and nanoindentation was performed on the bulk metallic glass (BMG) Vit106a ($Zr_{58.5}Cu_{15.6}Ni_{12.8}Al_{10.3}Nb_{2.8}$) to examine spatial mechanical property fluctuations, along the longitudinal and transverse faces of the specimen. The data gathered from the modulus mapping were the modulus maps as well as the complex modulus, E_r^* , which is a sum of the storage, E_r' , and loss, E_r'' , moduli. The data gathered from the nanoindenter were the reduced moduli, E_r , and the hardnesses, H , of the sample on the three faces. Collectively, mechanical heterogeneities were revealed.

2. MATERIALS AND METHODS

The Vit106a BMG specimen used in this research was created by casting the liquid alloy in a copper mold to produce the approximately 3mm x 10mm BMG plate. In order to properly analyze the mechanical properties on the three faces of the plate, proper polishing was quintessential and was a large part of the research. It is desirable to examine the materials properties of a specimen without damaging the material, hence careful polishing methods and techniques were utilized. The equipment used

to polish and examine the sample are listed in Table 1:

Table 1: Equipment Used for Polishing

Equipment	Purpose
Allied High Tech Products-MultiPrep System	Preparing samples for microscopic examination.
600, 800, 1200 Grit Silicon Carbide Paper	Various grit sandpaper for smooth finish.
Deionized Water	Cleaning sandpaper during polishing.
50% 0.02 μ m Colloidal Silica, 50% Water Solution	Final polishing grit for specimen.
Branson 2510 Ultrasonic Cleaner	Cleaning and removing particulates from sample.
Nikon Eclipse LV150N Microscope	For viewing sample surface under various magnifications.

To begin with, the specimen needed to be properly mounted to a metal disk to be placed onto the MultiPrep System for polishing. This was done by placing a small drop of Loctite 430 instant adhesive on a metal disc and then by carefully placing the specimen on top and allowing it to cure for at least 5 minutes. The first face that was polished was the longitudinal face as shown in Fig. 1 below:

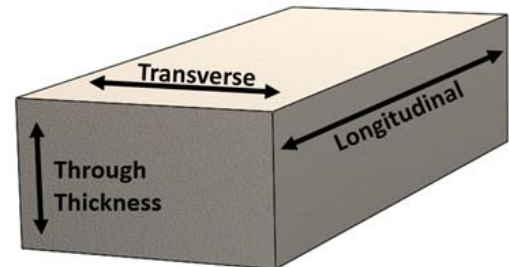


Figure 1: Orientation of Vit106a Sample

Since the first face that was polished was the longitudinal face, this means that the opposing longitudinal face was mounted to the metal disk. Once the sample was properly cured onto the mounting disk, the disk was placed onto the MultiPrep system and was first polished at 600 grit for 5 minutes. Next it was polished with 800 grit for 10 minutes, then 1200 grit for 30 minutes and then the very fine 0.02 μm colloidal silica polish for 1 hour. The higher the grit means the finer the finish. 600 grit translates to 30 μm , 800 grit translates to 25 μm and 1200 grit translates to 15 microns. After the final polishing of the sample with the colloidal silica, the sample was placed into a beaker of methanol which was then placed into the Branson cleaner to remove the colloidal silica particulates which conglomerate and stick to the surface of the specimen. The sample was sonicated in methanol for approximately 15 minutes, or until there were no visible colloidal silica particles when viewed under the Nikon microscope. Images of the various polishing stages are shown in Fig. 2-6, in section 3 of this paper.

This process of mounting and polishing was repeated for the next two transverse surfaces of the sample after direct modulus mapping and nanoindentation were performed on the surface that was just polished. The equipment used for performing the direct modulus mapping and nanoindentation are show in Table 2 below:

Table 2: Equipment Used for Property Testing

Equipment	Purpose
Bruker's Hysitron TI 950 TriboIndenter	Modulus mapping and nanoindentation of sample.
Diamond Berkovich Nanoindenter Tip	Used for modulus mapping and nanoindentation of sample.

The first process performed on the TriboIndenter was the direct modulus mapping. The DMM combines both scanning probe microscopy (SPM) with dynamic mechanical analysis to map the indentation modulus on the sample's surface. During this mapping, a sinusoidal load function was applied such that contact was constantly made between the diamond tip and the surface of the BMG specimen.[4] The maximum load was 5000 μN for all three mapping experiments that were conducted. This process allowed for determination of the storage modulus, E_r' , which can be calculated from the Eq. 1:

$$E_r' = \sqrt{\frac{k'^3}{6F_D r}} \quad (1)$$

where k' is the indentation storage stiffness, F_D is the dynamic load, and r is the radius of curvature of the Berkovich tip. The indentation storage stiffness, k' , can be calculated from Eq. 2:

$$k' = \frac{F_D \cos \theta}{d_D} + m_T \omega^2 - k_T \quad (2)$$

where d_D is the dynamic displacement, m_T is the mass of the force transducer, ω is the angular frequency and k_T is the stiffness of the force transducer.

The storage modulus, E_r' , is a measure of the elastic response of the material and measures the stored energy of the sample. This value is different than the Young's modulus and is considered to be the in-phase component. [5] The out of phase component is called the loss modulus, E_r'' , which measures the viscous response of the material. These two values summed together give rise to the complex modulus, E_r^* . The complex modulus maps for all three specimens are shown in Fig 8 in section 3.2.

The second process performed on the TriboIndenter was the nanoindentation. The nanoindentation was performed on the modulus mapped area in 4 regions and the reduced moduli, E_r , and the hardness, H , were recorded. The reduced modulus, E_r , is calculated from eq. 3:

$$E_r = \frac{S\sqrt{\pi}}{2\sqrt{A}} \quad (3)$$

where S is the stiffness of the unloading curve and A is the projected contact area. The reduced modulus is able to be related to the Young's modulus by eq. 4:

$$\frac{1}{E_r} = \frac{1 - \nu^2}{E_{sample}} + \frac{1 - \nu^2}{E_{indenter}} \quad (4)$$

where ν^2 is the Poisson ratio.

The way in which the hardness of the specimen was calculated was from eq. 5:

$$H = \frac{P_{max}}{A} \quad (5)$$

where P_{max} is the maximum indentation load and A is the resultant projected contact area at that specific load.

The final reduced modulus values are shown in tables 2 and 3 in section 3.3.

3. RESULTS AND DISCUSSION

3.1 Polishing

Proper polishing of the sample specimens was a very time consuming, but very crucial part of the process of preparing the Vit106a BMG sample for data collection on the nanoindenter. All three faces of the specimens started out with a polish at 600 grit which was

very rough and created large scratches. The grits were increased to remove these scratches and create a finer surface. The roughnesses were decreased from 600 grit to 800 grit to 1200 grit and then to a final polish with the 0.02 μm colloidal silica. Another reason why it is very important to prepare the surfaces carefully is because when mounting the specimen to a disc, the other faces will acquire glue build up. This first transverse face researched had acquired glue from when the first face, the longitudinal face, was mounted to the disc. Shown below in Fig 2 is an example of a face at 5x magnification that has had no preparation to it:

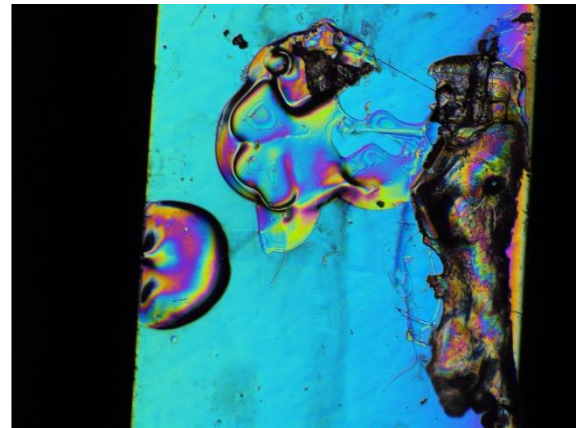


Figure 2: Before Polish, Face 2, 5x

Before moving onto polishing this face, a very careful removal of the glue without scratching the surface was required. In order to remove the glue, the sample was placed into a beaker filled with acetone and was then placed into the Branson Ultrasonic Cleaner until most of the glue was removed. After this step, the sample was mounted to the metal disc and was prepared for the first polish at 600 grit. An example of a 600 grit polish for 5 minutes at 5x magnification is shown below in Fig. 3:

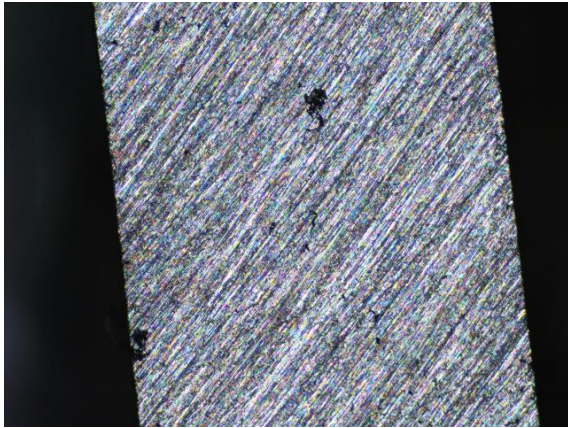


Figure 3: 600 Grit Finish, 5x, Face 3

Before being able to move onto the next fine grit size, it was crucial to make sure that there were uniform scratches for that grit. This image reveals a very uniform 600 grit polish. Since there were uniform scratches, this meant it was time to move onto the 800 grit. Shown below in Fig. 4 is an example of an 800 grit polish at 5x magnification:

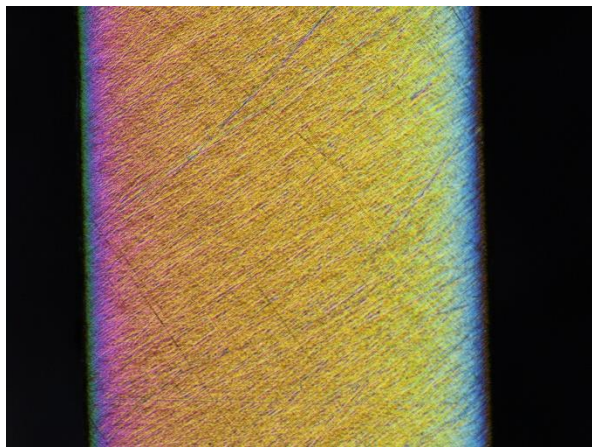


Figure 4: 800 Grit Finish, 5x, Face 3

It can be seen that this 800 grit finish reveals very fine scratches and has removed the vast majority of the 600 grit scratches. There are still a few 600 grit scratches left on the sample but considering that this specimen is approximately 3mm in width and the areas tested for modulus mapping and nanoindentation were on the micron scale, this is not a huge issue. After polishing at 800 grit

for a specific face, the next grit utilized was 1200 grit. Shown below in Fig. 5 is an example of a 1200 grit finish at 5x magnification:

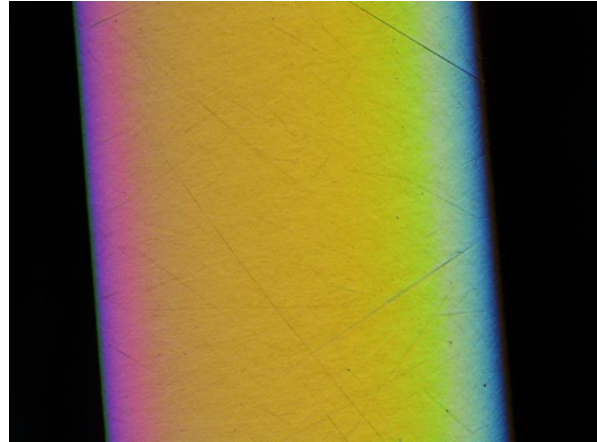


Figure 5: 1200 Grit Finish, 5x, Face 3

The 1200 grit finish is very fine and reveals other deeper scratches that were not easily visible at an 800 grit polish. The final polish with the colloidal silica is shown below in Fig. 6 with 10x magnification:

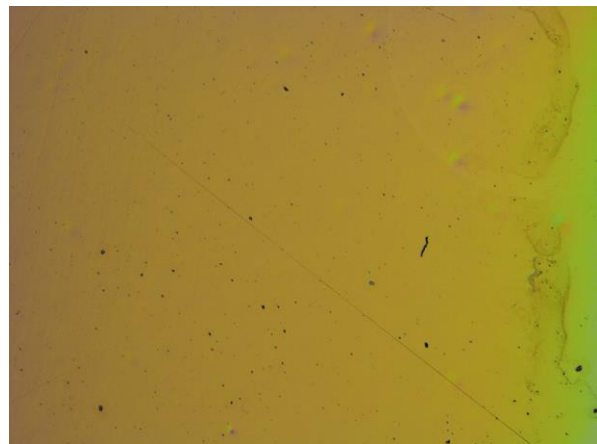


Figure 6: Colloidal Silica Finish, 10x, Face 1

This picture of the final finish for face 1 reveals that there were minimal scratches. A few scratches were inevitable, but this was not an issue as the modulus mapping and nanoindentation could avoid these regions. Achieving an even better finish through other methods may be desirable in the future.

3.2 Direct Modulus Mapping

Prior to bringing the specimen to the nanoindenter for modulus mapping, the sample was carefully removed from the metal disc that it was polished on by placing it into acetone and sonicating. After the sonication process, the sample was then very carefully picked up with tweezers and was mounted onto another metal disc, that was much thinner, to be placed into the nanoindenter for testing.

Through SPM, the nanoindenter probed the surface of the specimen to create a topological map in a predefined micron area. For the longitudinal face, face 1, a 10 x 10 micron region was defined. For the two transverse faces, faces 2 and 3, a 5 x 5 micron region was defined. Shown below in Fig. 7 is a picture of the topological image that was created by the DMM of the three faces:

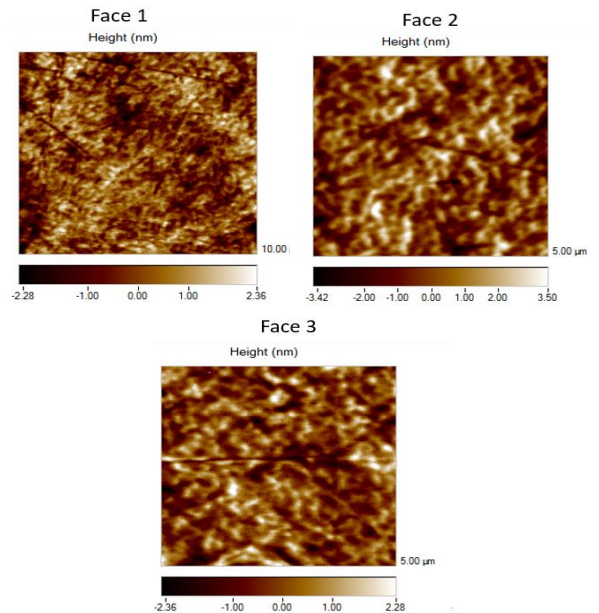


Figure 7: SPM Topography

It can be seen that for face 1, a very clean region was found as it does not appear to have any scratches. Face 2 also does not appear to have any scratches. When scanning various regions for face 3, it was determined

that the region was used was the best that was found. After the collection of the data it appeared that there may have been a scratch through the middle of this sample.

In addition to the DMM performing SPM for the topography of the faces, the DMM collected data on the complex moduli of the samples. The complex moduli of the three faces are shown below in Fig. 8:

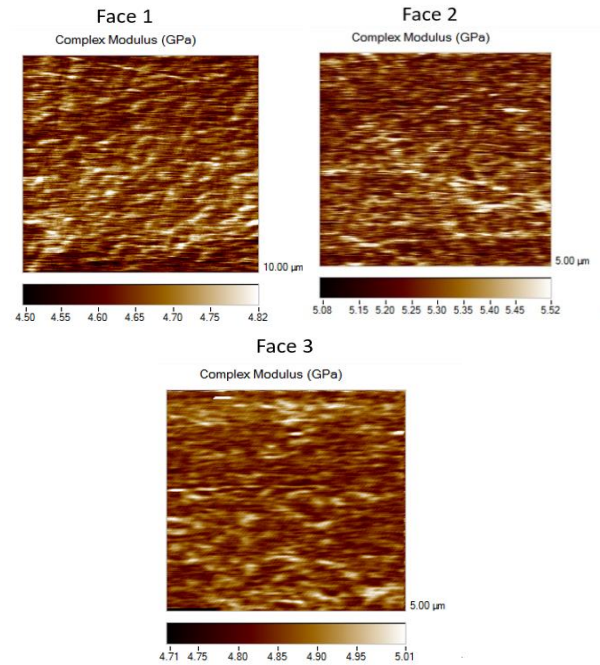


Figure 8: Complex Modulus Maps

The complex modulus maps across all three faces revealed structured variations in the complex moduli. In face 1 there was a gradient of complex moduli from 4.02 to 4.50 GPa. In face 2 there was a gradient of complex moduli ranging from 5.08 to 5.52 GPa. In face 3 there was a gradient of complex moduli ranging from 4.71 to 5.01 GPa. These variations appear to be structured but are still slightly difficult to see. A MATLAB code was developed by Peter Tsai to further categorize these complex moduli into defined regions and further reveal their heterogenous

microstructure. Shown below in Fig. 9 are K-Means maps of the three faces:

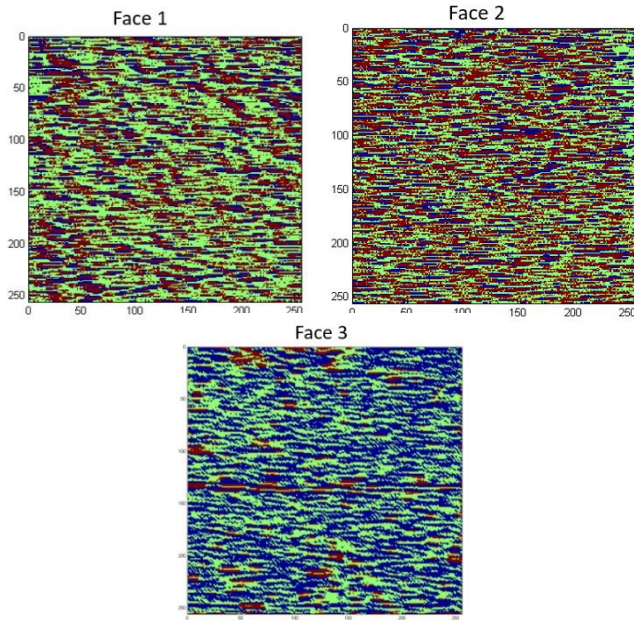


Figure 9: K-Means

The K-means map reveals clustering by categorizing the elastic microstructures of the three faces. The red region is the compliant modulus region, the blue region is the intermediate modulus region and the green region is the stiffest modulus region. Face 1 very clearly reveals a heterogeneous microstructure whereas faces 2 and 3 do appear to have structure but there is more noise. One potential reason for this issue is that the sample region for faces 2 and 3 was 5 x 5 microns, as opposed to the 10 x 10 microns for face 1.

To follow up with the K-Means map, a histogram was created to show the overlap of the complex moduli for the three faces. The deconvolved histogram is shown in Fig. 10:

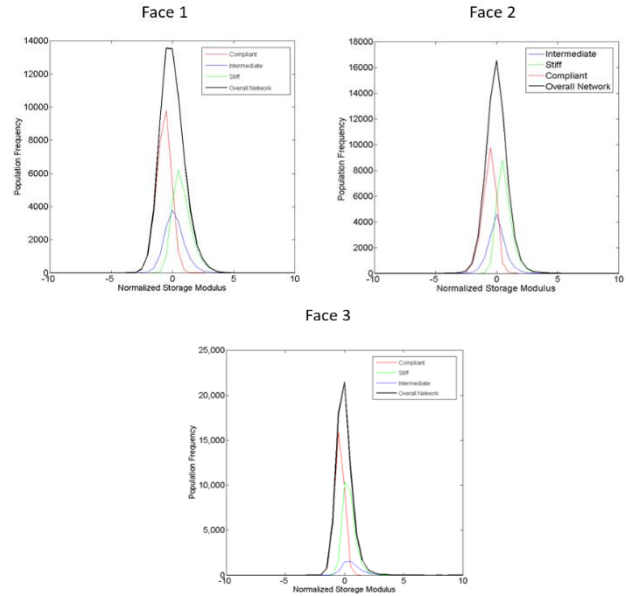


Figure 10: Deconvolved Histograms

The deconvolved histograms show the percent deviation from the mean complex modulus which is shown in black. For all three faces, the compliant, intermediate and stiff regions tend to align well and have similar population frequencies. Face 3 seems to be the outlier, and this may be due to the fact that there could have been a scratch across the middle of the sample, or that there was unprecedented noise affecting the nanoindenter.

3.3 Nanoindentation

After performing the DMM on the sample, nanoindentation was performed in the mapped regions. The nanoindentation revealed the storage modulus, Er' , and the hardness, H , of the three faces. The nanoindentation was performed while using a maximum applied load of 5000 μm . A 3D map created by the Triboscan software of an indent is shown below in fig. 11:

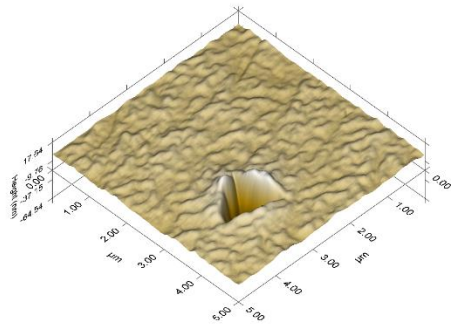


Figure 11: Nanoindent in Face 2

This 3D plot of the nanoindent provides a good visualization as to how the surface of the Vit106a BMG deforms under indentation. This image also provides a good visualization of the actual surface of a polished specimen.

Shown below in Fig. 12 is an example of the four nanoindents that were performed on all three faces of the sample.

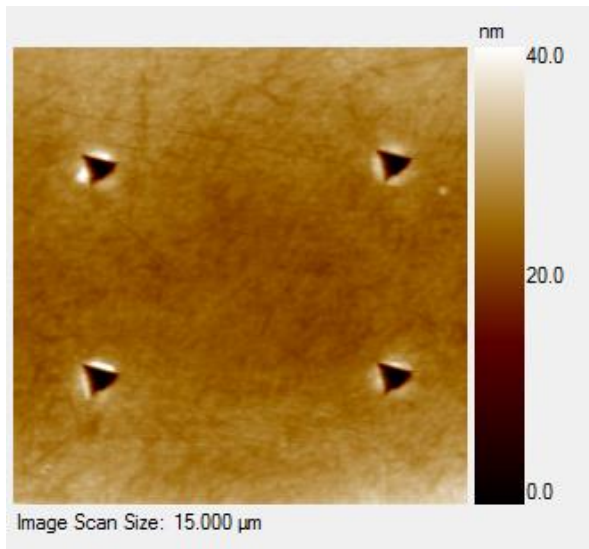


Figure 11: Nanoindents in Face 1

Four nanoindents were performed in order to show the variation in the storage modulus in the micron regions. The storage moduli and hardnesses collected are shown in Tables 1 and 2:

Table 2: Reduced Moduli and Hardnesses

Face	E_r (GPa)	H (GPa)
1a	68.47	5.10
1b	67.01	5.03
1c	67.88	5.02
1d	68.40	5.01
2a	68.88	5.16
2b	67.32	5.45
2c	66.12	5.17
2d	66.36	5.20
3a	71.45	5.01
3b	69.77	5.00
3c	71.28	4.97
3d	69.94	4.99

Table 3: Average Reduced Moduli and Hardnesses

Face	Avg. E_r (GPa)	Avg. H (GPa)
1	67.94	5.04
2	67.17	5.25
3	70.61	4.99

It is interesting to note that the moduli and hardnesses varies in such a small region, which is comparable to the variation in the results found in the DMM. Both the DMM and nanoindentation are suggestive of heterogenous elastic microstructures. Also, the complex moduli found from DMM have values very close to the hardnesses found from nanoindentation, which suggests a strong correlation between the two.

4. Conclusion

Normally, you do not have structure in amorphous BMGs, but because of the way this sample was casted, elastic microstructures were revealed through DMM and nanoindentation of this Vit106a specimen. Phase separation clearly occurred for this specimen. Potential areas to consider for future study are performing DMM and nanoindentation on the through-thickness surface of the specimen and comparing to the

transverse sections. Also, paying closer attention to exactly how the sample was processed and casted may reveal that the structure varies as a function of cooling the sample. Current research has shown that there are other ways to cure the BMG other than casting in a mold, such as casting in a vacuum and even more precisely, casting in a high vacuum electrostatic levitator.[1]

ACKNOWLEDGEMENTS

I thankfully acknowledge the support from Dr. Katharine Flores and all group members in the Flores Research Group, including Porter Weeks, Mu Li, and Juan Wang. I also thankfully acknowledge the support from Washington University as all of the data was collected within the facilities of the Institute of Materials Science and Engineering.

REFERENCES

- [1] W. Johnson, “Metallic Glasses: Science and Technology,” 14-Oct-2016.
- [2] W. L. Johnson, J. H. Na, and M. D. Demetriou, “Quantifying the origin of metallic glass formation,” *Nat. Commun.*, vol. 7, no. 1, Apr. 2016.
- [3] J. Schroers, “Bulk Metallic Glass: The Smaller the Better,” *Adv. Mater.*, vol. 23, no. 4, pp. 461–476, Jan. 2011.
- [4] P. Tsai, K. Kranjc, and K. M. Flores, “Hierarchical heterogeneity and an elastic microstructure observed in a metallic glass alloy,” *Acta Mater.*, vol. 139, pp. 11–20, Oct. 2017.
- [5] “Dynamic Mechanical Analysis (DMA) A Beginner’s Guide,” p. 23.